Geophys. J. R. astr. Soc. (1980) **60**, 187–207

Estimate of wind stressed sea level excitation of the Earth's annual wobble

William P. O'Connor *Department of Meteorology and Center for Climatic Research, Institute for Environmental Studies, University of Wisconsin, Madison, Wisconsin 53706, USA*

Received 1979 June 18; in original form 1978 August 13

Summary. This article estimates the contribution to the Earth's annual wobble caused by the wind stressed non-isostatic sea level variations in the oceans. Since there is a lack of data on these sea level changes, an analytic approach is taken. An ocean basin is assumed to be bounded by two meridians of longitude and two parallels of latitude, and is symmetric about the equator. A simple zonal wind stress profile based on observed data represents the seasonal changes in each hemisphere with a simple annual cosine variation. The one layer barotropic ocean has a frictionally controlled boundary layer giving rise to a western boundary current. From the equations of motion a stream function and vorticity equation are developed. The ocean is assumed to be always in adjustment to the wind stress forcing so that the steady state solution yields the velocity and height fields. Model parameters are adjusted so that these sea level changes correspond to estimates of non-isostatic sea level changes.

The expression for the annual height field changes caused by the wind stress forcing is substituted into the equations governing the wobble excitation. From the resulting expression it is seen that for an ocean basin and wind regime symmetric about the equator, the contributions to the excitation of wobble from the northern and southern oceans add, while the contributions to the length of day cancel.

The pole of excitation for the resultant of all oceans moves along an ellipse of eccentricity unity (line segment), aligned nearly along the Greenwich meridian, with semi-major axes of 19 cm, and is farthest from the pole of reference along 11° E longitude in mid-February. This indicates that the major contribution to the sea level excitation comes from the set up in the western Pacific. The positive annual frequency vector is calculated to be $(1.2-0.8i)\times 10^{-8}$ rad. Comparisons with the results of Wilson & Haubrich (1976a) show that this wind stressed sea level excitation of wobble is of the phase and probable magnitude to significantly reduce the discrepancy

between the astronomically observed excitation and the calculated geophysical excitations due to air mass redistribution, continental water storage and mountain torque.

1 Introduction

There is a seasonal redistribution of atmospheric mass and oceanic mass (set up caused by wind stress) which changes the moment of inertia tensor of the atmosphere and ocean. Because the total angular momentum of the Earth–atmosphere–ocean system is conserved, the Earth must compensate for this changing mass distribution in the atmosphere and ocean. This causes the Earth's annual wobble, so that the North Pole moves in an approximate ellipse with axes of about 4 m. The observed wobble has two components, with an annual and the 14 month Chandler period, which corresponds to the Eulerian period of free nutation for the elastic Earth. This article will consider only the annual period. A thorough explanation of the Earth's wobble and detailed development of the equators governing the wobble excitation are given in the treatise by Munk & MacDonald (1960).

The position of the pole of rotation is determined by astronomical observation and the necessary excitation function forcing the wobble can subsequently be calculated. The excitation function caused by a geophysical event can be calculated from geophysical data. The major forcing of the annual wobble is the seasonal variation in atmospheric mass over Eurasia and the northern hemisphere oceans. However, this does not account for all of the wobble, as determined by comparisons of the amplitude and phase of this atmospheric excitation with the amplitude and phase of that excitation necessary to account for the observed annual wobble (Sidorenkov 1973). Further studies considering additional effects of winds, ocean currents, and seasonal ground water storage on the continents have failed to completely reconcile the geophysical wobble excitation with the observed annual wobble excitation (Wilson & Haubrich 1976a).

The problem of determining the mass distribution in the oceans which excites wobble is a difficult one. The ocean responds nearly as an inverted barometer to atmospheric pressure, i.e. the ocean surface is depressed 1 cm for every excess millibar of atmospheric pressure. Also, steric sea level changes occur due to changes in temperature and salinity above the thermocline. These sea level fluctuations due to pressure and temperature are called isostatic, because the total air and water mass above that point on the Earth does not change (except for a small annual variation since more air mass is over continents in the northern hemisphere winter), and so no excitation of wobble occurs. It is only the non-isostatic, or uncompensated, sea level changes forced by the wind stress than can excite wobble. Since the annual sea level changes are nearly isostatic (Lisitzin 1974; Pattullo *et al.* 1955), it is difficult to determine the wind stressed sea level from data records.

As stated by Munk & MacDonald, and reiterated by Wilson & Haubrich, the excitation of wobble due to the wind stressed non-isostatic sea level changes is one of the remaining problems related to the Earth's rotation. The aim of this article is to estimate this effect. Because of a lack of data on seasonal non-isostatic sea level changes, a simple analytical model is developed in Section 2. This model is similar to those developed to explain the major features of ocean circulation on a beta plane as a result of wind stress forcing, except that here the sphericity of the Earth is retained. In Section 3 the model is compared with what data are available, so that reasonable seasonal sea level changes will be used. In Section 4 the analytical expression for the wind stressed sea level changes is substituted into the wobble equations, and the excitation due to this seasonal shift in ocean mass is calculated. Finally, in Section 5 the path of the excitation pole and positive annual frequency vector of

the ocean excitation are calculated and compared with those of other geophysical excitations.

2 Analytic solution for wind stressed sea level

The problem is to determine the annual change in sea level that is forced by the wind stress. For simplicity we consider an ocean basin that is symmetric about the equator, bounded by two meridians of longitude and two parallels of latitude. The barotropic ocean is taken to be of constant density and constant depth, in its undisturbed state. Following Stommel (1948) and Veronis (1966) we will consider only a linearized form of bottom friction which will be important in balancing the pressure gradient force and coriolis force in the western boundary current. The ocean is taken to be effectively incompressible. Since we have only a one layer fluid model, we integrate the equations of motion, so that the velocity represents and average one for the layer. The linearized equations for horizontal momentum and mass conservation are:*

$$\frac{\partial u}{\partial t} = -\frac{g}{a\cos\phi}\frac{\partial \eta}{\partial \lambda} + 2\Omega v \sin\phi - Ku + \frac{1}{D}\frac{\tau_x}{\rho} \tag{1}$$

$$\frac{\partial v}{\partial t} = -\frac{g}{a}\frac{\partial \eta}{\partial \phi} - 2\Omega u \sin\phi - Kv + \frac{1}{D}\frac{\tau_y}{\rho} \tag{2}$$

$$\nabla \cdot \mathbf{v} = \frac{1}{a\cos\phi}\left[\frac{\partial u}{\partial \lambda} + \frac{\partial}{\partial \phi}(v\cos\phi)\right] = 0. \tag{3}$$

The zonal wind stress forcing has its longitudinal and latitudinal dependence represented by the separable form

$$\frac{\tau_x}{\rho} = T_x G(\lambda) E(\phi, t), \tag{4}$$

where the value of the dimensional constant is $T_x = 1\ \mathrm{cm^2\ s^{-2}}$. The expression

$$G(\lambda) = \frac{1}{2}\left(1 + \sin\frac{\lambda\pi}{\lambda_0}\right) \tag{5}$$

gives a sinusoidal variation which has its minima at the longitudinal boundaries $\lambda = 0, \lambda_0$, and reaches its maximum at mid-ocean. This longitudinal variation is constant in time. We represent the latitudinal variation of the zonal wind stress with only an annual sinusoidal variation in time. The time of maximum wind stress is taken to be mid-February ($t' = \nu t = 1/8$) for the northern hemisphere and mid-August ($t' = \nu t = 5/8$) for the southern hemisphere. This profile is then determined by a sixth-order interpolating polynomial

$$E(\phi, t) = c_1\phi^6 + c_2\phi^5 + c_3\phi^4 + c_4\phi^3 + c_5\phi^2 + c_6\phi + c_7 \tag{6}$$

* Symbols defined in an appendix.

subject to the constraints

$$E(\phi_0, t) = T_0 + \Delta T_0 \cos(2\pi\nu t - \pi/4) \tag{7}$$

$$E(-\phi_0, t) = T_0 - \Delta T_0 \cos(2\pi\nu t - \pi/4) \tag{8}$$

$$\frac{\partial E}{\partial \phi}(\phi_0, t) = 0 \tag{9}$$

$$\frac{\partial}{\partial \phi} E(-\phi_0, t) = 0 \tag{10}$$

$$E(0, t) = -T_E \tag{11}$$

$$E(\phi_m, t) = -T_m - \Delta T_m \cos(2\pi\nu t - \pi/4) \tag{12}$$

$$E(-\phi_m, t) = -T_m + \Delta T_m \cos(2\pi\nu t - \pi/4) \tag{13}$$

where

$\phi_0 = 50°$

$\phi_m = 20°$

$T_0 = 1$

$T_m = 0.4$

$T_E = 0.5$

$\Delta T_0 = 0.25$

$\Delta T_m = 0.15$.

The motivation for this expression may be seen from Fig. 1 which shows the seasonal variation in $E(\phi, t)$. For simplicity, the wind regime assumed for this study is symmetric about the equator for the respective seasons in each hemisphere, which occur six months apart. We note that conditions (9) and (10) require that the curl of the wind stress vanish on the northern and southern boundaries. The expression for $E(\phi, t)$ is determined from conditions (7)–(13) by solving seven simultaneous linear algebraic equations. The resulting

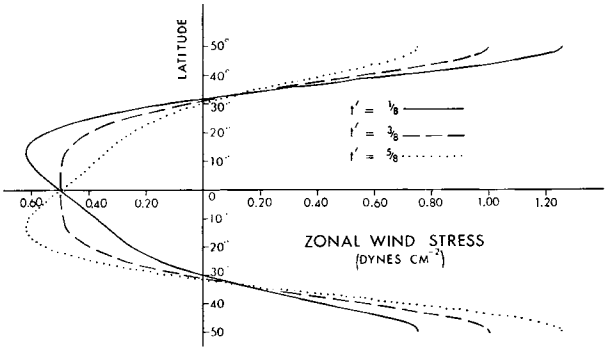

Figure 1. Latitudinal variation of zonal wind $E(\phi, t)$ assumed for February ($t' = 1/8$), May ($t' = 3/8$) and August ($t' = 5/8$).

constants are found to be

$c_1 = -6.851$

$c_2 = \bar{c}_2 \cos(2\pi\nu t - \pi/4), \quad \bar{c}_2 = -2.044$

$c_3 = 7.848$

$c_4 = \bar{c}_4 \cos(2\pi\nu t - \pi/4), \quad \bar{c}_4 = 2.925$

$c_5 = -0.03387$

$c_6 = \bar{c}_6 \cos(2\pi\nu t - \pi/4), \quad \bar{c}_6 = -0.7558$

$c_7 = -0.5.$

The resulting zonal wind stress profile equation (4) over the ocean basin is shown in Fig. 2. This profile was chosen to generally resemble those seasonal zonal wind stress values given by Hellerman (1967), but subject to our constraint that the curl vanish on the northern and southern boundaries of our closed ocean basin. We have chosen to neglect the meridional wind stress by setting $\tau_y = 0$. This will be discussed further later. Since this is an analytic model with many simplifying assumptions, the purpose is not to duplicate identically the observational wind stress data, but to create a wind field that reproduces the major features of the seasonal variation in the tropical easterlies and mid-latitude westerlies in both hemispheres.

	60°W	50°	40°	30°	20°	10°	0°
50°N	62	94	117	125	117	94	62
45°	54	80	100	107	100	80	54
40°	34	51	64	68	64	51	34
35°	13	19	24	26	24	19	13
30°	-06	-09	-11	-12	-11	-09	-06
25°	-19	-29	-36	-39	-36	-29	-19
20°	-28	-41	-51	-55	-51	-41	-28
15°	-31	-46	-57	-62	-57	-46	-31
10°	-31	-46	-57	-61	-57	-46	-31
5°	-28	-42	-53	-56	-53	-42	-28
0°	-25	-37	-47	-50	-47	-37	-25
5°	-22	-33	-41	-44	-41	-33	-22
10°	-19	-28	-35	-38	-35	-28	-19
15°	-16	-24	-30	-32	-30	-24	-16
20°	-13	-19	-23	-25	-23	-19	-13
25°	-08	-11	-14	-15	-14	-11	-08
30°	00	00	00	00	00	00	00
35°	10	14	18	19	18	14	10
40°	21	32	40	43	40	32	21
45°	32	48	60	64	60	48	32
50°S	37	56	70	75	70	56	38

Figure 2. Zonal wind stress profiles ($\tau_x \times 10^{-2}$ dyne cm^{-2}) assumed for model Atlantic Ocean in February ($t = 1/8$).

The two dimensional, incompressible form of the continuity equation allows us to define a stream function

$$u = -\frac{\partial \psi}{\partial \phi}, \qquad v = \frac{1}{\cos \phi} \frac{\partial \psi}{\partial \lambda}. \tag{14}$$

We eliminate the surface height from equations (1) and (2) by forming a vorticity equation. With the aid of equation (14) we obtain the linear inhomogeneous vorticity equation for the stream function

$$\frac{\partial}{\partial t} \nabla^2 \psi + K \nabla^2 \psi + 2\Omega \frac{\partial \psi}{\partial \lambda} = -\frac{1}{\rho D \cos \phi} \frac{\partial}{\partial \phi} (\tau_x \cos \phi) \tag{15}$$

where the non-dimensional Laplacian operator is defined by

$$\nabla^2 = \frac{1}{\cos^2 \phi} \frac{\partial^2}{\partial \lambda^2} + \frac{1}{\cos \phi} \frac{\partial}{\partial \phi} \left(\cos \phi \frac{\partial}{\partial \phi} \right). \tag{16}$$

The boundary conditions on ψ are determined from the conditions that the normal component of velocity must vanish at the boundary, so that the boundary is a streamline ($\psi = 0$, at $\lambda = 0, \lambda_0$ and $\phi = \phi_0, -\phi_0$). We define the non-dimensional (primed) variables

$$t = \frac{1}{\nu} t', \qquad \psi = \frac{T_x}{\Omega D} \psi' \tag{17}$$

so that t' varies from 0 on January 1 to 1 on December 31. We substitute equation (4) into equation (15) and proceed to non-dimensionalize this equation to obtain

$$\frac{\nu}{2\Omega} \frac{\partial}{\partial t'} \nabla^2 \psi' + \epsilon \nabla^2 \psi' + \frac{\partial \psi'}{\partial \lambda} = \frac{-G(\lambda)}{2 \cos \phi} \frac{\partial}{\partial \phi} [\cos \phi E(\phi, t)] \tag{18}$$

where $\epsilon = K/2\Omega$ represents the magnitude of the frictional influence.

Since we are only interested in the annual sea level fluctuations which excite the Earth's wobble (as opposed to higher frequency surface waves), we shall require our solution to have only the annual period, as does the forcing. This represents a considerable mathematical simplification of the problem and may be justified by noting that the annual variation in the wind stress forcing is much slower than the period of adjustment of the ocean to the imposed forcing (a few weeks at most). This can also be seen by comparing magnitudes of the non-dimensional coefficients in equation (18). The value $\nu/2\Omega \approx 2 \times 10^{-4}$ is an order of magnitude smaller than ϵ (which will subsequently be calculated in a boundary layer analysis). Then the ocean is in a steady state balance to the wind stress forcing, and the mathematical solution to the time dependent problem can be represented by the solution to the steady state problem, with the forcing allowed to vary with the annual period. The stream function equation is now

$$\epsilon \nabla^2 \psi' + \frac{\partial \psi'}{\partial \lambda} = \frac{-G(\lambda)}{2 \cos \phi} \frac{\partial}{\partial \phi} [\cos \phi E(\phi, t)]. \tag{19}$$

It is our desire to match the solution for the boundary layer with that in the central ocean where friction can be neglected. The frictionless form ($\epsilon = 0$) of equation (19) shows that in the central ocean there is a balance between the advection of planetary vorticity and the curl of the wind stress. This solution is found by integrating equation (19) with respect

to λ, and using equation (5), to obtain

$$\psi' = -\frac{1}{4}\left[\lambda - \frac{\lambda_0}{\pi}\cos\frac{\lambda\pi}{\lambda_0}\right]\frac{1}{\cos\phi}\frac{\partial}{\partial\phi}\left[\cos\phi\, E(\phi, t)\right] + F_1(\phi). \tag{20}$$

Following Veronis (1966) we proceed with a boundary layer analysis by assuming that

$$\frac{\partial}{\partial\lambda} = \epsilon^n \frac{\partial}{\partial\xi},$$

so that equation (19) becomes

$$\frac{\epsilon^{2n+1}}{\cos^2\phi}\frac{\partial^2\psi'}{\partial\xi^2} + \frac{\epsilon}{\cos\phi}\frac{\partial}{\partial\phi}\left(\cos\phi\frac{\partial\psi'}{\partial\phi}\right) + \epsilon^n\frac{\partial\psi'}{\partial\xi} = -\frac{1}{4}\left[1 + \sin\left(\frac{\xi\pi}{\epsilon^n\lambda_0}\right)\right]\frac{1}{\cos\phi} \tag{21}$$

$$\times \frac{\partial}{\partial\phi}\left[\cos\phi\, E(\phi, t)\right].$$

If $n > 0$, the left side is at most $O(\epsilon)$ and no term can balance the right side. If $n < -1$, the first term on the left dominates and there is no boundary layer. We choose n so that the first and third terms balance, and so $n = -1$. This gives the equation

$$\frac{1}{\cos^2\phi}\frac{\partial^2\psi'}{\partial\xi^2} + \frac{\partial\psi'}{\partial\xi} = O(\epsilon). \tag{22}$$

The solution to the homogeneous form is

$$\psi' = H_1(\phi)\exp\left(-\frac{\lambda}{\epsilon}\cos^2\phi\right) + F_2(\phi). \tag{23}$$

The total approximate solution to equation (19) is the sum of the frictionless equation (20) and boundary layer equation (23) solutions,

$$\psi' = H_1(\phi)\exp\left(-\frac{\lambda}{\epsilon}\cos^2\phi\right) - \frac{1}{4}\left[\lambda - \frac{\lambda_0}{\pi}\cos\frac{\lambda\pi}{\lambda_0}\right]\frac{1}{\cos\phi}\frac{\partial}{\partial\phi}\left[\cos\phi\, E(\phi, t)\right] + F_3(\phi) \tag{24}$$

Because we chose the curl of the wind stress to vanish at the northern and southern boundaries, we can satisfy the boundary conditions (to within $O(\epsilon)$) by choosing $H_1(\phi)$ and $F_3(\phi)$ so that $\psi' = 0$ at $\lambda = 0, \lambda_0$. The approximate stream function is found to be

$$\psi' = -\frac{1}{4}\left[\lambda - \lambda_0 - \frac{\lambda_0}{\pi}\left(1 + \cos\frac{\lambda\pi}{\lambda_0}\right) + \lambda_0\left(1 + \frac{2}{\pi}\right)\exp\left(-\frac{\lambda}{\epsilon}\cos^2\phi\right)\right]$$

$$\times \frac{1}{\cos\phi}\frac{\partial}{\partial\phi}\left[\cos\phi E(\phi, t)\right]. \tag{25}$$

We define a non-dimensional sea level height η' by

$$\eta = \frac{aT_x}{gD}\eta' \tag{26}$$

With the use of equations (4), (14), (17) and (26) we may write the steady state horizontal momentum equations (1) and (2) in their non-dimensional form

$$2 \sin \phi \frac{\partial \psi'}{\partial \lambda} = \frac{\partial \eta'}{\partial \lambda} - \cos \phi E(\phi, t) G(\lambda) \tag{27}$$

$$2 \sin \phi \frac{\partial \psi'}{\partial \phi} = \frac{\partial \eta'}{\partial \phi} + \frac{2\epsilon}{\cos \phi} \frac{\partial \psi'}{\partial \lambda} \tag{28}$$

where we have neglected $\epsilon u'$ because it is small everywhere (in the boundary layer $\lambda \approx \epsilon$).

We integrate these equations to obtain η'. Integrating equation (27) with respect to λ we obtain

$$2 \sin \phi \, \psi' = \eta' - \frac{1}{2}\left[\lambda - \frac{\lambda_0}{\pi} \cos \frac{\lambda \pi}{\lambda_0}\right] \cos \phi E(\phi, t) + F(\phi). \tag{29}$$

Substituting the stream function expression (25) on the right of equation (28), neglecting terms of $O(\epsilon)$, and then integrating with respect to ϕ we obtain

$$2 \sin \phi \, \psi' = \eta' - \frac{1}{2}\left[\lambda - \lambda_0 - \frac{\lambda_0}{\pi}\left(1 + \cos \frac{\lambda \pi}{\lambda_0}\right)\right] \cos \phi E(\phi, t) + H(\lambda). \tag{30}$$

Equating equations (29) and (30) we obtain the function $F(\phi)$, and observe that the separation of variables requires that the function H be a constant or at most a function of time. When $F(\phi)$ is then substituted into equation (29), the resulting expression for the non-dimensional sea level heights is found to be identical to equation (30) except that now H is a constant or function only of time. Substituting the stream function expression (25) into (30) we obtain

$$\eta' = -\frac{1}{2}\left[\lambda - \lambda_0 - \frac{\lambda_0}{\pi}\left(1 + \cos \frac{\lambda \pi}{\lambda_0}\right) + \lambda_0 \left(1 + \frac{2}{\pi}\right) \exp\left(-\frac{\lambda}{\epsilon} \cos^2 \phi\right)\right]$$

$$\times \tan \phi \frac{\partial}{\partial \phi} [\cos \phi E(\phi, t)] + \frac{1}{2}\left[\lambda - \lambda_0 - \frac{\lambda_0}{\pi}\left(1 + \cos \frac{\lambda \pi}{\lambda_0}\right)\right] \cos \phi E(\phi, t) + H, \tag{31}$$

which satisfies equations (27) and (28) to within $O(\epsilon)$. We note that when the polynomial (6) for $E(\phi, t)$ is substituted into equation (31) those resulting coefficients of $\cos(2\pi t' - \pi/4)$ are odd functions of ϕ, while those terms that do not vary in time are even functions of ϕ. This is what we would expect from the nature of the wind stress forcing. The seasonal oscillation in set up would be antisymmetric about the equator, superimposed on a basic east to west set up that is symmetric about the equator.

To evaluate the function H we impose the requirement that the ocean mass be conserved at any instant of time so that the integral of the sea level departures from the undisturbed state vanishes when the integration is carried out over the ocean basin. This is expressed by the condition

$$\int_0^{\lambda_0} \int_{-\phi_0}^{\phi_0} \eta' \cos \phi \, d\phi \, d\lambda = 0. \tag{32}$$

We note that there still can be an average wind stressed sea level set up about which there is a seasonal oscillation. We proceed to substitute equation (31) into equation (32) and carry out

the integration. We note that after integration in λ the exponential term in equation (31) is of $O(\epsilon)$ and can subsequently be neglected. The expression (6) for the interpolating polynomial $E(\phi, t)$ is then substituted, and the result is found to be

$$H = -\frac{\lambda_0}{\sin\phi_0}\left(\frac{1}{2}+\frac{1}{\pi}\right)\int_0^{\phi_0}[\sin\phi\cos\phi\,(6c_1\phi^5+4c_3\phi^3+2c_5\phi)-(c_1\phi^6+c_3\phi^4+c_5\phi^2+c_7)]\,d\phi$$

$$= -\frac{\lambda_0}{\sin\phi_0}\left(\frac{1}{2}+\frac{1}{\pi}\right)(0.695). \tag{33}$$

We note that this 'correction tide' term H is not a function of time, because the coefficients of $\cos(2\pi t' - \pi/4)$ in equation (32) were odd functions of ϕ and vanished when integrated over latitude. Physically this comes about because the seasonal wind stress profile is symmetric about the equator in the respective seasons, with the wind stress value at the equator constant in time.

We observe that if the ocean is bounded by the meridians of longitude $\lambda = \lambda_i, \lambda_0$, the above results are valid provided that λ is replaced by $\lambda - \lambda_i$ and λ_0 is replaced by $\lambda_0 - \lambda_i$. Then by substituting equation (33) into equation (31), and making use of equation (26) we may write the wind stressed sea level changes for an ocean bounded by meridians λ_i and λ_0 in the form

$$\eta(\lambda,\phi,t) = \frac{aT_x}{gD}\left\{-\frac{1}{2}\left[\lambda-\lambda_0-\frac{(\lambda_0-\lambda_i)}{\pi}\left(1+\cos\frac{\lambda-\lambda_i}{\lambda_0-\lambda_i}\pi\right)\right.\right.$$

$$\left.+(\lambda_0-\lambda_i)\left(1+\frac{2}{\pi}\right)\exp\left(-\frac{(\lambda-\lambda_i)}{\epsilon}\cos^2\phi\right)\right]\times\tan\phi\,\frac{\partial}{\partial\phi}[\cos\phi\,E(\phi,t)]$$

$$+\frac{1}{2}\left[\lambda-\lambda_0-\frac{(\lambda_0-\lambda_i)}{\pi}\left(1+\cos\frac{\lambda-\lambda_i}{\lambda_0-\lambda_i}\pi\right)\right]\cos\phi\,E(\phi,t)$$

$$\left.-\frac{(\lambda_0-\lambda_i)}{\sin\phi_0}\left(\frac{1}{2}+\frac{1}{\pi}\right)(0.695)\right\}. \tag{34}$$

3 Comparison of analytic and observed results

We have yet to determine an appropriate value of the parameter ϵ. From equation (19) we see that in the boundary layer we have the approximate balance of terms

$$\epsilon\nabla^2\psi' \approx \frac{\partial\psi'}{\partial\lambda}, \tag{35}$$

and there the longitudinal gradients are much larger than the latitudinal gradients

$$\frac{\partial\psi'}{\partial\lambda} \gg \frac{\partial\psi'}{\partial\phi}, \tag{36}$$

from which we obtain the result that

$$\frac{\partial}{\partial\lambda} \approx \frac{\cos^2\phi}{\epsilon} \approx \frac{1}{\epsilon}. \tag{37}$$

We shall tune our ocean model to the Atlantic. We assume the northern boundary is at $\phi_0 = 50°$. As pointed out by Veronis (1965, 1966), the ratio of the width of the Gulf Stream to the width of the Atlantic is about 1/100. Then we have

$$\frac{\Delta\lambda}{\lambda_0} = \frac{\epsilon}{\lambda_0} = 0.01. \tag{38}$$

Taking $\lambda_0 = 60°$ for the angular width of the Atlantic we arrive at $\epsilon = 0.01$ when calculations are made in radians. This justifies the approximation made in dropping the first term of equation (18).

The meridional velocity is obtained from equation (25) with the use of equations (14) and (17). The angular width of the western boundary current λ_w is then obtained by setting $v = 0$ to obtain, approximately

$$\lambda_w = \frac{\epsilon}{\cos^2\phi} \ln\left[\frac{\lambda_0}{\epsilon}\left(1+\frac{2}{\pi}\right)\cos^2\phi\right]. \tag{39}$$

The mass transport of the boundary current (ignoring sea level changes since $\eta \ll D$) is, approximately

$$M = \rho D \int_0^{\lambda_w} v\cdot(a\cos\phi)\,d\lambda = \frac{T_x \rho a}{\Omega}\,\frac{\lambda_0}{4}\left(1+\frac{2}{\pi}\right)\frac{1}{\cos\phi}\,\frac{\partial}{\partial\phi}\left[\cos\phi\, E(\phi, t)\right] \tag{40}$$

which, we note, does not depend on the depth. This is the same result found in numerical models by Gates (1972) provided that the ocean depth represents some characteristic depth of frictional influence of the wind stress (on the order of several hundred metres). From equations (25) and (31) we also observe that the shape of the stream-function and height field contours does not depend on the depth. The value of ϵ was varied until the shape of the stream-function and height field contours appeared reasonable, and a representative value is $\epsilon = 0.005$. The maximum boundary current mass transport occurs near latitude $\phi = 36°$, where the curl of the wind stress has a maximum. Here the angular width of the boundary current is about $\lambda_w = 2.4°$, and the maximum mass transport varies seasonally from 9.1 to 17.2×10^{12} g s^{-1}.

The mass transport is smaller by about a factor of two from the values obtained by both analytic beta plane models (Munk 1950; Vernois & Morgan 1955) and from global ocean barotropic numerical circulation models using constant density and constant depth (Bryan & Cox 1972; Bye & Sag 1972; Holland & Hirschman 1972). These numerical investigations indicate that baroclinic processes and bottom topography greatly influence the resulting mass transport of the model. The maximum mass transport of the Gulf Stream occurs near latitude 35° N and is estimated to be $70–80 \times 10^{12}$ g s^{-1}. As discussed by Stommel (1965, p. 19) it is difficult to compare mass transports of models with observational data, chiefly because the assumed depth at which motion vanishes is difficult to determine with certainty. Another factor making comparisons difficult is that in the real ocean the currents are influenced by baroclinic effects and bottom topography as well as the wind stressed barotropic set up. For this reason it would be difficult to obtain the non-isotropic mass distribution directly from current measurements.

Although the shape of the velocity and height field contours does not depend on ocean depth, the magnitudes are inversely proportional to the depth. This was also the case with models by Gates (1972) and Veronis & Morgan (1955), who then were able to adjust their annual sea level fluctuations by varying the ocean depth. From equation (34) we see that the

sea surface slope is inversely proportional to the constant depth. It is precisely this feature that will allow us to estimate the wind stressed sea level changes from scarce observational data, and the subsequent effect on the Earth's wobble. The whole of Section 2 was devoted to obtaining an analytic model with a reasonable shape to its height field. If sufficient observational data on the seasonal wind stressed non-isostatic sea level variations were available, one could use an appropriate interpolation scheme and no dynamical model would be necessary. Since this is not the case, our dynamical model must serve the function of an interpolation scheme. We do this by adjusting the model depth D until the maximum annual sea level change of the model corresponds to the maximum annual non-isostatic sea level change that we estimate for the western Atlantic. In effect, a simple barotropic model is used to represent the seasonal non-isostatic ocean set up which may be influenced by more complicated baroclinic processed (including the variation in thermocline depth) in the real ocean. This rests on the assumption that the wind stressed non-isostatic set up in the real ocean has a height field pattern that is similar to that pattern derived in the analytic model.

The information we need is the seasonal change in the bottom pressure, the total mass change on the ocean floor due to mass changes of the ocean and atmosphere above. Calculations were made by Gill & Niiler (1973, Fig. 3) which gave a maximum seasonal change of bottom pressure in the western Atlantic and Pacific equivalent to changes of 1 and 4 cm of non-isostatic sea level, respectively. Recently published data from the Mid Ocean Dynamics Experiment (Brown *et al.* 1975, Fig. 5) indicates that seasonal bottom pressure fluctuations in the western Atlantic near Bermuda may be on the order of several millibars. (1 cm of water load is the pressure equivalent of 1 mbar.) Furthermore, these bottom pressure fluctuations are attributed to the ocean response to changing wind stress, and not simply to the local changes in atmospheric pressure. At present only a few months of data are available from stations near Bermuda.

We must make an estimate of the non-isostatic sea level changes in order to calibrate our model. Obviously, the wobble excitation depends critically on the magnitude chosen for the seasonal change in non-isostatic sea level. The sea level data available from island stations probably shows the dynamics of the wind stress on the ocean basins better than the data from coastal stations. From the study by Pattullo *et al.* (1955, Chart 1) the indications are that the annual non-isostatic sea level variation at island stations in the mid-latitude western Atlantic is about 7 cm. Accordingly, the ocean depth $D = 800$ m gives a seasonal oscillation of about 7.8 cm with the wind stress profiles assumed above. The difference in sea level height between winter and summer for our model of the North Atlantic is shown in Fig. 3. The results may be compared with the calculations of Gill & Niiler (1973, Fig. 3) which show a pattern of maximum non-isostatic set up in the western North Atlantic and Pacific in winter, but of smaller magnitude.

This model with its boundary current and height field support is qualitatively similar to the rectangular beta plane models of Kenyon (1975, Figs 1 and 2), who also used a separable form of the wind stress curl which vanished on the northern and southern boundaries. We recall that we neglected the meridional wind stress. We could have included a representation of meridional wind flow giving convergence in the tropics and poleward flow in mid-latitudes with a meridional wind stress profile varying only as a function of latitude, $\tau_y = \tau_y(\phi)$. Such a meridional profile would contribute nothing to the wind stress curl and therefore not enter into the calculation of the stream function or mass transport, but would only enter into the calculation of the height field using the horizontal momentum equations. Work with this model shows that the effect of including a meridional wind stress would be to decrease the set up at mid-latitudes by a centimetre or two (and subsequently this has only a minor effect on the wobble excitation).

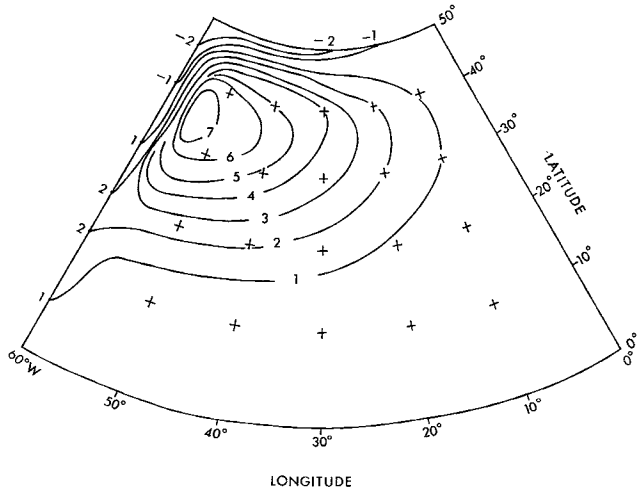

Figure 3. Difference in wind stressed sea level between winter ($t' = 1/8$) and summer ($t' = 5/8$) for North Atlantic Ocean model. Isopleths are in centimeters. Mass is conserved because the sea level differences in the South Atlantic are the negative of the mirror images about the equator.

In order to tune our model to the North Pacific, we assume the longitudinal width is 120°, the latitudinal width is still from 50° N to 50° S, and assume $\epsilon = 0.01$. (In actual practice, the model is not extremely sensitive to changes in the value of ϵ as long as it still is of the order of magnitude to represent the scale of the western boundary current in the ocean.) As determined by Hickey (1975), island stations in the western equatorial Pacific show an annual sea level change of about 10 cm, with the maximum occurring in late winter or spring, despite the fact that the ocean temperature is near its minimum at this time. This indicates that the sea level change is primarily the result of wind stress forcing. It is not an exact measurement of the non-isostatic set up because there is compensation in the mass distribution due to vertical displacement of the thermocline. In any case, we shall assume that the wind stressed non-isostatic set up in the Pacific is about the same as that found in the Atlantic. In our model, by assuming a Pacific Ocean depth $D = 1600$ m, we obtain a seasonal oscillation of 8.0 cm with our same wind stress profiles.

4 The excitation function

The coordinate system is that used in previous studies by Munk & MacDonald and Wilson & Haubrich. The origin of a complex plane is at the mean position of the North Pole, called the pole of reference, the real axis x_1 is along the Greenwich meridian, and the imaginary axis x_2 is along the 90° E longitude meridian. The vertical axis x_3 is parallel to the Earth's mean rotational axis. The instantaneous position of the North Pole, $\mathbf{m}(t) = m_1(t) + im_2(t)$, called the pole of rotation, is related to the instantaneous position of the pole of excitation $\Psi(t) = \Psi_1(t) + i\Psi_2(t)$, representing the geophysical forcing of the wobble, by the equation

$$\frac{i}{\sigma_0}\frac{d}{dt}\mathbf{m} + \mathbf{m} = \Psi. \tag{41}$$

In calculating the excitation function Ψ we follow Munk & MacDonald and assume that the excitation due to relative angular momentum changes (motion) can be neglected compared to excitation due to changes in mass distribution, because the least motion required to effect the mass changes is small compared to the observed motion. In any case, the wobble excitation due to ocean currents is small because these currents are nearly in geostrophic balance, and geostrophic motion does not excite wobble. Wilson & Haubrich estimate the excitation due to ocean currents to be three orders of magnitude smaller than significant meteorological excitations.

Since the only excitation we are considering is the redistribution of ocean mass which loads the Earth (Munk & MacDonald 1960, p. 42) we assume that the increase in excitation due to rotational deformation is balanced by the decrease in excitation due to load deformation, so that the resulting Ψ in our equations is that for a rigid earth. In calculating the variation in length of day (lod), our value of Ψ_3 would have to be multiplied by the transfer coefficient 0.7 because of load deformation.

With the above assumptions, the excitation function for a changing mass distribution near the Earth's surface is given by Munk & MacDonald (1960, p. 106). In this study the ocean mass redistribution is given solely by the changes in sea level so that the excitation function for an ocean can be written

$$\Psi = -\frac{a^4\rho}{C\text{-}A}\int_{-\phi_0}^{\phi_0}\int_{\lambda_i}^{\lambda_0}[\eta(\phi,\lambda,t)-\bar{\eta}(\phi,\lambda)]\cos^2\phi\sin\phi\exp(i\lambda)\,d\lambda\,d\phi, \tag{42}$$

$$\Psi_3 = -\frac{a^4\rho}{C}\int_{-\phi_0}^{\phi_0}\int_{\lambda_i}^{\lambda_0}[\eta(\phi,\lambda,t)-\bar{\eta}(\phi,\lambda)]\cos^3\phi\,d\lambda\,d\phi. \tag{43}$$

where we have used the latitude ϕ instead of the co-latitude.

In keeping with the traditional notation we let $\odot = 2\pi t'$ be the longitude of the mean Sun which varies from 0° on January 1 to 360° on December 31. Then the annual variation may be expressed as

$$\cos\left(\odot-\frac{\pi}{4}\right)=\frac{1}{\sqrt{2}}(\cos\odot+\sin\odot). \tag{44}$$

We proceed to evaluate the excitation function for the set up in an ocean basin. From equation (34) and the $\cos(\odot-\pi/4)$ variation of terms in equation (6), we see that the average sea level height $\bar{\eta}$ occurs at $\odot = 3\pi/4, 7\pi/4$, so that $\bar{\eta}$ contains only those terms of equation (34) that do not depend on time. At these times the wind stress profile $E(\phi, t)$ is symmetric about the equator so that the seasonal set up in both hemispheres vanishes and only the constant east to west set up remains. Therefore the expression $\eta - \bar{\eta}$ depends only on those terms that are coefficients of $\cos(\odot-\pi/4)$, because all other terms, including the correction tide, subtract out. When equation (34) is substituted into equation (42), the resulting expressions in λ can be integrated by parts. Subsequently it is seen that the exponential term, when integrated, is of $O(\epsilon)$ and can be neglected. Use is made of equation (44) so that the results are expressible in terms of the linear components of the excitation function

$$\Psi_1 = C_1\cos\odot + D_1\sin\odot \tag{45}$$

$$\Psi_2 = C_2\cos\odot + D_2\sin\odot \tag{46}$$

where

$$C_1 = D_1 = \frac{-1}{\sqrt{2}} \frac{a^5 \rho T_x}{gD(C\text{-}A)} \Phi \cdot \frac{1}{2} \left\{ (\lambda_0 - \lambda_i) \sin \lambda_i + \cos \lambda_0 - \cos \lambda_i - \frac{(\lambda_0 - \lambda_i)}{\pi} \right.$$
$$\left. \times \left[\sin \lambda_0 - \sin \lambda_i - \frac{\sin \lambda_0 + \sin \lambda_i}{1 - [\pi^2/(\lambda_0 - \lambda_i)^2]} \right] \right\} \tag{47}$$

$$C_2 = D_2 = \frac{-1}{\sqrt{2}} \frac{a^5 \rho T_x}{gD(C\text{-}A)} \Phi \cdot \frac{1}{2} \left\{ (\lambda_i - \lambda_0) \cos \lambda_i + \sin \lambda_0 - \sin \lambda_i - \frac{(\lambda_0 - \lambda_i)}{\pi} \right.$$
$$\left. \times \left[\cos \lambda_i - \cos \lambda_0 + \frac{\cos \lambda_0 + \cos \lambda_i}{1 - [\pi^2/(\lambda_0 - \lambda_i)^2]} \right] \right\} \tag{48}$$

and

$$\Phi = \int_{-\phi_0}^{\phi_0} \sin \phi \cos \phi \{ - \sin \phi \cos \phi (5\phi^4 \bar{c}_2 + 3\phi^2 \bar{c}_4 + \bar{c}_6) + \phi^5 \bar{c}_2 + \phi^3 \bar{c}_4 + \phi \bar{c}_6 \} d\phi = -0.1543. \tag{49}$$

We have noted that the terms in the integrand involving the boundary layer parameter ϵ occurring in the height field have been dropped, because after the integration by parts in λ they are seen to be of $O(\epsilon)$. This is because ϵ, as it appears in the stream function, is only important in the boundary layer, which is small compared to the entire ocean. Although ϵ does not appear explicitly in the excitation function, we should keep in mind that its effect has occurred in a more roundabout way: ϵ sets the scale of frictional influence and the width of the boundary layer, which effects the shape of the contours and spacing of the streamlines, which determines the necessary height field support, which was adjusted to the desired magnitude by changing the value of D which appears explicitly in the excitation function. The values for the Atlantic and Pacific oceans are shown in Table 1.

From equations (47)–(49) we observe that for a mass distribution that is antisymmetric about the equator, as the wind stressed set up is at any instant of time, the integrals of ϕ in the wobble excitation equations are even functions. The result is that for an ocean basin symmetric about the equator (as the Atlantic and Pacific might be thought of as being) and for similar wind regimes in the hemispheres, the wobble excitation Ψ is twice that value it would be for each northern or southern ocean basin by itself.

This is in contrast to the lod excitation. When equation (34) is substituted into equation (43) the resulting integrals of ϕ are odd functions and vanish when integrated over latitude.

Table 1. Model ocean parameters.

Ocean	D (m)	λ_i ($^\circ$ long)	λ_0 ($^\circ$ long)	ϕ_0 ($^\circ$ lat)	ϵ	Maximum change in set up (cm)*
Atlantic	800	60W	0	50	0.005	7.8
Pacific	1600	140E	100W	50	0.01	8.0
Indian	800	40E	100E	50	0.005	7.8

*This is the maximum seasonal change in nonisostatic sea level in the western boundary current near 36° latitude: $\max|\eta(t' = 1/8) - \eta(t' = 5/8)|$ for ocean.

The result is that for an ocean basin symmetric about the equator, with symmetric wind regimes, the contributions from the northern and southern oceans cancel each other and there is no excitation of the lod. In fact, changing ocean mass distributions have only a small effect on the lod compared to the relative angular momentum changes arising from changing winds. The seasonal variation in lod is the result of a near cancellation between winter wind regimes in the hemispheres (Munk & MacDonald 1960, p. 125). It is perhaps interesting that seasonal changes in the lod are due to near cancellation between the winter regimes of the hemispheres for both winds and non-isostatic water distributions. Because of this near cancellation in the lod excitation the existing data are probably not sufficient to make an accurate calculation of Ψ_3 with this model. The discussion of the lod excitation was included only for completeness and we shall not pursue the matter further.

In fact, the ocean basins are not symmetric about the equator, and the southern hemisphere winds are stronger than those in the northern hemisphere. Furthermore, in the southern hemisphere the oceans are not bounded on the south, but instead there is complete circumpolar flow, so that water can flow around the continents and our assumption of a bounded ocean is not fulfilled. Also, here the curl of the wind stress does not vanish at the southern boundary, i.e. the maximum westerly winds do not necessarily occur at the latitude of the southernmost extent of the continents. The thermal equator does not coincide with the geographical equator, but instead shifts position with the seasons. All this would be exceedingly difficult to include in an analytic model treating each of the oceans individually. Even a more empirical approach would be difficult because the limited sea level data available comes primarily from the northern hemisphere oceans. For the above reasons we have assumed that the southern hemisphere oceans are reflections about the equator of the nothern hemisphere ones. The fact that the northern and southern ocean contributions both act to increase (as opposed to cancel) the wobble excitation, may serve as a justification of this approximation.

We now make an estimate of the wobble excitation due to the Indian Ocean. Our analytic model with its resulting cross equatorial flow does not apply to this ocean, since most of it lies in the southern hemisphere. However, we can make a simple estimate by making use of the model result that for an ocean basin symmetric about the equator, the wobble excitation is twice that value of each northern or southern basin by itself. Hence if we assume a 'virtual' Indian Ocean lies north of the equator, we may obtain an estimate with our model. We assume that this 'virtual' Indian Ocean has the same latitudinal and longitudinal width, depth and boundary parameter ϵ as the Atlantic Ocean, but is displaced in longitude to conform to geography (Table 1). We then take only half the magnitude of the resulting excitation.

5 Comparison of geophysical and observed excitations

From the linear components of the excitation function we may proceed to analyse the results. We now choose to express the excitation function in the alternate form of circular components (Munk & MacDonald 1960, p. 47).

$$\Psi = \Psi^+ \exp(i\odot) + \Psi^- \exp(-i\odot) = |\Psi^+| \exp[i(\odot + \lambda^+)] + |\Psi^-| \exp[-i(\odot - \lambda^-)] \tag{50}$$

where

$$\Psi^+ = \tfrac{1}{2}[(C_1 + D_2) + i(C_2 - D_1)] \tag{51}$$

$$\Psi^- = \tfrac{1}{2}[(C_1 - D_2) + i(C_2 + D_1)]. \tag{52}$$

In general this describes elliptical motion of the excitation pole with semi-major axes $|\Psi^+| + |\Psi^-|$, and semi-minor axes $|\Psi^+| - |\Psi^-|$. Since this study uses only the simple annual time variation $\cos(\odot - \pi/4)$, we have the case of plane polarization $|\Psi^+| = |\Psi^-|$, and the excitation pole moves back and forth in a straight line segment corresponding to the major axis of an ellipse with eccentricity unity. The path of the excitation pole is oriented along east longitude $\frac{1}{2}(\lambda^+ + \lambda^-)$, where

$$\lambda^+ = \arg \Psi^+ = \arctan\left(\frac{C_2 - D_1}{C_1 + D_2}\right) \tag{53}$$

$$\lambda^- = \arg \Psi^- = \arctan\left(\frac{C_2 + D_1}{C_1 - D_2}\right). \tag{54}$$

These values have been computed for the oceans and are given in Table 2. Generally the path of the excitation pole for each ocean is aligned along a meridian running through the western part of that ocean basin. The pole of excitation is farthest from the reference pole in mid-February, $\odot = \pi/4$ and mid-August, $\odot = 5\pi/4$. In mid-February for both northern and southern hemisphere oceans, the excitation pole is on the meridian that is 180° opposite to that one through the ocean basin (Table 2). At this time the ocean set up is greatest in the northern hemisphere, and least in the southern hemisphere because of the reversal of seasons, and both conditions shift the pole of excitation in the same direction, in accordance with conservation of angular momentum.

The excitation for the Atlantic Ocean has a semi-major axis of 22 cm, while that for the Pacific has the value of 41 cm. The excitation pole for the resultant of all oceans is oriented nearly along the Greenwich meridian, with semi-major axis of 19 cm and is farthest from the pole of reference along 11° E longitude at $\odot = \pi/4$. This indicates that a major contribution to the sea level excitation comes from the set up in the western North and South Pacific. This may be compared with the significantly larger excitation due to the seasonal shift in air mass over Asia, which has a semi-major axis of 120 cm, and is farthest from the pole of reference along 80° E longitude at $\odot = 0°$ (Sidorenkov).

From the development of Munk & MacDonald (1960, pp. 47, 94) we note that although the positive and negative annual excitations Ψ^+ and Ψ^- may be of the same order of magnitude for a geophysical excitation, Ψ^+ is better determined than Ψ^-. This is because the annual excitation frequency is close to the Chandler resonance frequency, so that the positive component of the rotation pole is about 10 times the magnitude of the negative component, and it is from these astronomically observed values of the pole position that the resultant excitation due to all geophysical excitations must be calculated. This means that the length of the semi-major axis of the excitation ellipse is better determined than the semi-minor axis or the eccentricity. For this reason Wilson & Haubrich compared estimates of the

Table 2. Wobble excitation parameters for oceans (units of 10^{-8} rad unless otherwise stated).

Ocean	C_1, D_1	C_2, D_2	$\frac{C_1 + D_2}{2}$	$\frac{C_2 - D_1}{2}$	$\frac{C_1 - D_2}{2}$	$\frac{C_2 + D_1}{2}$	semi-major axis (cm)	$\frac{\lambda^+ + \lambda^-}{2}$ (°E. long) at $\theta = \pi/4$
Atlantic	-1.85	1.61	-0.12	1.73	-1.73	-0.12	22	139
Pacific	4.50	-0.18	2.16	-2.34	2.34	2.16	41	-2 (2°W)
Indian	-0.63	-1.05	-0.84	-0.21	0.21	-0.84	11	59
All Oceans	2.02	0.38	1.20	-0.82	0.82	1.20	19	11

Table 3. Positive circular excitation vectors from Wilson & Haubrich (1976a, Table 2) (units of 10^{-8} rad).

Excitation		Data Source	$\underline{\Psi}^+$	$\underline{X}^+ - \underline{\Psi}^+$
Air Mass (IB = Inverted Barometer)	1 a	NCAR IB	-1.7 -5.3i	
	b	Rand IB	-1.2 -4.5i	
	c	Sidorenkov IB	-1.9 -9.1i	
	d	Rand local-IB	-2.7 -5.6i	
	e	Rand non-IB	-1.9 -8.2i	
Mountain torque	2	NCAR	0.1 +0.4i	
Water Storage	3	Van Hylckama	2.4 +2.4i	
Wind Stressed Sea Level	4	This study	1.2 -0.8i	
	5 a	1a + 2 + 3	0.8 -2.5i	2.9 -4.4i
	b	1c + 2 + 3	0.6 -6.3i	3.1 -0.6i
	c	1d + 2 + 3	-0.2 -2.8i	3.9 -4.1i
	d	1e + 2 + 3	0.6 -5.4i	3.1 -1.5i
$\underline{\Psi}^+$	6 a	4 + 5a	2.0 -3.3i	1.7 -3.6i
	b	4 + 5b	1.8 -7.1i	1.9 +0.2i
	c	4 + 5c	1.0 -3.6i	2.7 -3.3i
	d	4 + 5d	1.8 -6.2i	1.9 -0.7i
$\underline{X}^+$	7	ILS 1901-1970	3.7 -6.9i	

positive annual frequency components due to geophysical excitations Ψ^+ with that value X^+ determined by astronomical observations of the International Latitude Service (ILS 1901–1970) reported by Vicente & Yumi (1969, 1970).

In order that we may compare the wind stressed sea level excitation with other geophysical and observed excitations, the positive annual frequency components given by Wilson & Haubrich (1976a, Table 2) are included here in Table 3. Their estimates of the total geophysical excitation were made by using the water storage on the continents (Van Hylckama 1956, 1970), wind excitation calculated from mountain torques (Wilson & Haubrich 1976b), and several estimates of the air mass excitation (Wilson & Haubrich 1976a, References). These air mass excitation calculations were made by assuming inverted barometer, non-inverted barometer, and local inverted barometer response of the oceans. In the case of the local inverted barometer response, the average pressure anomaly over an ocean basin is used in place of the local pressure anomaly. With this assumption water does not flow between ocean basins. Their results showed that the air mass excitations using the non-inverted barometer and local inverted barometer hypotheses are larger than the excitation using the inverted barometer hypothesis. Wilson & Haubrich thought that their study underestimated the air mass excitation over Asia due to a lack of data and their interpolation scheme, and that Sidorenkov's air mass estimate was probably the most accurate. The closest estimate of Ψ^+ to X^+ was found by using the Sidorenkov inverted barometer air mass excitation. The next best estimate was found using air mass excitation from Rand Corporation data with the non-inverted barometer hypothesis for the ocean. Estimates giving larger discrepancies were found using air mass excitations from NCAR data with the inverted barometer hypothesis, and Rand data with the local inverted barometer hypothesis for ocean basins. Their results are shown graphically in Fig. 4.

Wilson & Haubrich concluded that the discrepancy between the observed and calculated excitations might be due to inaccurate estimates of air mass excitation, water storage on land, or non-isostatic water redistribution in the oceans. From Table 3 we see that our estimate of the positive annual frequency excitation for the wind stressed sea level changes is $(1.2-0.8i)\times 10^{-8}$ rad. When this estimate is added to those of the continental water

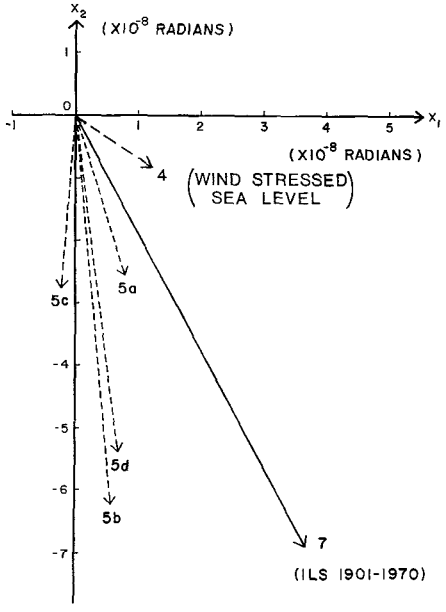

Figure 4. Positive circular annual excitation vector from geophysical estimates of air mass redistribution, continental water storage, and mountain torque (Wilson & Haubrich 1976a, Fig. 4), ILS data and the wind stressed sea level (this study). Numbers refer to lines in Table 3.

storage, mountain torque and various air mass excitations, the resultant Ψ^+ vector is always closer to the observed ILS value of X^+. In particular, the addition of this non-isostatic ocean excitation to the geophysical estimate made with the Sidorenkov air mass excitation gives a good approximation to the observed ILS excitation (Table 3 and Fig. 4).

Possibly the only previous estimate of the wobble excitation due to non-isostatic sea levels was made by Munk & MacDonald (1960, p. 122) based on the sea level study of Pattullo *et al.* (1955), which indicated that in April the northern hemisphere oceans have a deficit of water and the southern hemisphere oceans have a surplus. In computing the excitation due to these seasonal departures in ocean mass they assumed that the load departures were concentrated at four latitudes and obtained the values

$$\Psi_1 = (-9.8 \cos \odot - 5.4 \sin \odot) \times 10^{-8}$$

$$\Psi_2 = (-4.6 \cos \odot - 8.2 \sin \odot) \times 10^{-8}$$

from which we calculate that the excitation ellipse has a semi-major axis of 90 cm, a semi-minor axis of 25 cm, and is oriented so that the excitation pole lines on the semi-major axis at 39° E longitude in August and 141° W longitude in February. This is accordingly reflected in the value of the positive annual frequency component of $\Psi^+ = (-9.0 + 0.4i) \times 10^{-8}$. Their excitation pole found by estimating seasonal ocean load departures is nearly 180° out of phase with the excitation pole found in this study using the wind stressed set up. Munk & MacDonald (1960, p. 122) stated that their estimate of the seasonal ocean mass departures was so uncertain that the spring deficit might not really exist. This could be the cause of the discrepancy between our excitation functions.

This analytic study admittedly is a very simple approach to determine the wind stressed sea level excitation, but may be justified by the lack of data on non-isostatic sea level

changes. From equations (45)–(49) we see that it is the longitudinal and latitudinal ocean basin extent, ocean dynamics yielding a set up near the western boundary, and time of maximum in the annual cycle that determine the phase of Ψ^+, while the sea level changes specified by depth D and wind stress T_x determine the amplitude. The values of the non-isostatic sea level changes chosen may be somewhat arbitrary, but are probably of the same order of magnitude as the true values. The question of the magnitude of the non-isostatic sea level changes will probably be answered only when long period bottom pressure records become available from appropriate ocean locations. However, Gill & Niiler (1973) observe that point measurements might not be representative of large areas because local topography strongly influences the barotropic set up. They then suggest that gravimetric instruments could be located on islands in order to measure the loading of the Earth due to ocean bottom pressure changes. Then if these data indicate a significantly different set up from that assumed here, the magnitude of the excitation would have to be revised accordingly.

The conclusion that we then make from this study is that the wind stressed sea level excitation of wobble is of the phase and probable magnitude to significantly reduce the discrepancy between the observed excitation and the calculated geophysical excitations due to air mass redistribution, water storage on the continents and mountain torque.

Acknowledgments

The research reported here was accomplished as part of the PhD programme in the Meteorology Department, University of Wisconsin, Madison. The author wishes to thank Dr John A. Young, Professor of Meteorology, for his advice in the formulation of the problem of the ocean response to wind stress forcing. Dr Richard E. Meyer, Professor of Mathematics, aided in finding the boundary layer solution for the stream function and height fields. Dr David D. Houghton, Professor of Meteorology, pointed out the necessity of the correction tide to conserve mass. Two anonymous reviewers provided suggestions that improved the presentation of the article. The manuscript was typed by Ms Pat Klitzke and the figures were drawn by Mr Jeremiah N. Obiefuna and Ms Susan H. Smith. Funding for the computer calculations was made by the Center for Climatic Research, Institute for Environmental Studies, University of Wisconsin, under NSF Grant No. ATM74-23041.

References

Brown, W., Munk, W., Snodgrass, F., Mofjeld, H. & Zetler, B., 1975. MODE bottom experiment, *J. phys. Oceanogr.*, **5**, 75–85.

Bryan, K. & Cox, M., 1972. The circulation of the world ocean: a numerical study. Part 1, a homogeneous model, *J. phys. Oceanogr.*, **2**, 319–335.

Bye, J. & Sag, T., 1972. A numerical model for circulation in a homogeneous world ocean, *J. phys. Oceanogr.*, **2**, 305–318.

Gates, W., 1972. Numerical studies of transient planetary circulations in a wind-driven ocean, *Pure appl. Geophys.*, **99**, 169–200.

Gill, A. & Niiler, P., 1973. The theory of the seasonal variability in the ocean, *Deep Sea Res.*, **20**, 141–177.

Hellerman, S., 1967. An updated estimate of the wind stress on the world ocean, *Mon. Weath. Rev.*, **95**, 607–626. (Correction: 1968. **96**, 62–74.)

Hickey, B., 1975. The relationship between fluctuations in sea level, wind stress, and sea surface temperature in the equatorial Pacific, *J. phys. Oceanogr.*, **5**, 460–475.

Holland, W. & Hirschman, A., 1972. A numerical calculation of the circulation in the North Atlantic, *J. phys. Oceanogr.*, **2**, 336–354.

Kenyon, K., 1975. The influence of longitudinal variations in wind stress curl on the steady ocean circulation, *J. phys. Oceanogr.*, **5**, 334–346.

Lisitzin, E., 1974. *Sea Level Changes*, Elsevier, Amsterdam, 286 pp.

Munk, W., 1950. On the wind-driven ocean circulation, *J. Met.*, **7**, 79–93.

Munk, W. & MacDonald, G., 1960. *The Rotation of the Earth, a Geophysical Discussion*, Cambridge University Press, 323 pp.

Pattullo, J., Munk, W., Revelle, R. & Strong, E., 1955. The seasonal oscillation in sea level, *J. mar. Res.*, **14**, 88–155.

Sidorenkov, N., 1973. The inertia tensor of the atmosphere, the annual variation of its components, and the variations of the Earth's rotation, *Atmos. oceanic Phys.*, **9**, 185–192.

Stommel, H., 1948. The westward intensification of wind-driven ocean currents, *Trans. Am. geophys. Un.*, **29**, 202–206.

Stommel, H., 1965. *The Gulf Stream. A Physical and Dynamical Description*, University of California Press, 248 pp.

Van Hylckama, T., 1956. The water balance of the Earth, *Publs Clim. Drexel Inst. Technol.*, **9**, 57.

Van Hylckama, T., 1970. Water balance and earth unbalance, International Association of Scientific Hydrology, *Proc. Reading Symp. World Wat. Balance*, **2**, 434–444.

Veronis, G., 1965. On parametric values and types of representation in wind-driven ocean circulation studies, *Tellus*, **17**, 77–84.

Veronis, G., 1966. Wind-driven ocean circulation – Part 1. Linear theory and perturbation analysis, *Deep Sea Res.*, **13**, 17–29.

Veronis, G. & Morgan, G., 1955. A study of the time-dependent wind-driven circulation in a homogeneous, rectangular ocean, *Tellus*, **7**, 232–242.

Vicente, R. & Yumi, S., 1969. Co-ordinates of the Pole (1899–1968) referred to the Conventional International Origin, *Publs int. Latit. Obs. Mizusawa*, **7**, 41.

Vicente, R. & Yumi, S., 1970. Revised values (1941–1962) of the co-ordinates of the Pole referred to the CIO, *Publs int. Latit. Obs. Mizusawa*, **7**, 109.

Wilson, C. & Haubrich, R., 1976a. Meteorological excitation of the Earth's wobble, *Geophys. J. R. astr. Soc.*, **46**, 707–743.

Wilson, C. & Haubrich, R., 1976b. Atmospheric contributions to excitation of the Earth's wobble 1901–1970, *Geophys. J. R. astr. Soc.*, **46**, 745–760.

Appendix: list of symbols

A, C Moments of inertia of Earth.
$C = 8.068 \times 10^{44}$ g cm^2, $C\text{-}A = 2.6 \times 10^{42}$ g cm^2.

D Ocean depth at rest.

$C_1, D_1, C_2, D_2, C_3, D_3$ Linear components of excitation function.

$F(\phi, t)$ Zonal annual wind stress profile.

H Correction tide.

K Coefficient of bottom friction.

M Mass transport of boundary current.

O( ) Order of approximation.

T_x 1 cm^2 s^{-2}.

$\mathbf{X}^+$ Observed positive circular annual excitation vector.

a Mean radius of Earth 6.371×10^8 cm.

g Acceleration of gravity 980 cm s^{-2}.

$\mathbf{m} = m_1 + im_2$ Pole of rotation position.

t Time.

u Zonal velocity positive eastward.

v Meridional velocity positive northward.

$\mathbf{\Psi} = \Psi_1 + i\Psi_2$ Pole of (wobble) excitation position.

Ψ_3 Excitation of length of day.

$\mathbf{\Psi}^+$ Positive circular annual excitation vector.

Ψ^- Negative circular annual excitation vector.
Ω Earth's angular velocity 7.292×10^{-5} rad s^{-1}.
ϵ Frictional parameter.
η Sea level deviation from depth D.
λ Longitude.
λ_i Longitude of western ocean boundary.
λ_0 Longitude of eastern ocean boundary.
λ_w Angular width of boundary current.
λ^+ Argument of positive annual excitation vector.
λ^- Argument of negative annual excitation vector.
ν Annual frequency 3.18×10^{-8} rad s^{-1}.
ρ Density of water 1 g cm^{-3}.
σ_0 Chandler frequency $(2\pi/14)$ rad $month^{-1}$.
τ_x Zonal wind stress on ocean.
τ_y Meridional wind stress on ocean.
ϕ Latitude.
ϕ_0 Latitude of northern boundary of ocean.
ψ Stream function for ocean velocities.
$\odot$ Longitude of mean Sun (0° on January 1).